Articles

The Trimetallic Cation $[Hg_2Pt(CH_2P(S)Ph_2)_4]^{2+}$ in $[Hg_2Pt(CH_2P(S)Ph_2)_4]X_2$, X = BPh_4^-, PF_6^-. An Isoelectronic Analogue of $Au_2Pt(CH_2P(S)Ph_2)_4$

Thomas F. Carlson, John P. Fackler, Jr.,* Richard J. Staples, and Richard E. P. Winpenny

Department of Chemistry and Laboratory for Molecular Structure and Bonding, Texas A&M University, College Station, Texas 77843-3255

Received April 29, 1994[⊗]

A trimetallic Hg(II)−Pt(II)−Hg(II) complex, $[Hg_2Pt(CH_2P(S)Ph_2)_4]X_2$ (X = BPh_4, PF_6), was obtained from the reaction of $Hg(MTP)_2$ (MTP = $CH_2P(S)Ph_2$) with 1 equiv of $Pt[S(CH_2CH_3)_2]_2Cl_2$, in CH_2Cl_2, in the presence of either $NaBPh_4$ or $TlPF_6$. The X-ray crystal structures of these compounds show the ylide ligand bridging the three metals with Hg··Pt distances of 3.016(1) and 3.138(1) Å, respectively. In contrast to the isoelectronic and structurally similar $Au_2Pt(MTP)_4$ complex, the trimetallic cationic units are each nonlinear, with angles of 166.3-(1) and 149.1(1)° for the BPh_4^- and PF_6^- salts, respectively. Unlike $Au_2Pt(MTP)_4$, the mercury−platinum complex reacts with halogens to give Hg−C bond cleavage products. No materials are formed which contain Hg−Pt bonds. Crystallographic details for $[Hg_2Pt(CH_2P(S)Ph_2)_4](PF_6)_2 \cdot {}^1/_2C_2H_4Cl_2$ are as follows: triclinic space group $P\bar{1}$, a = 11.264(9) Å, b = 13.666(3) Å, c = 20.930(5) Å, α = 107.965(1)°, β = 94.548(1)°, γ = 94.848(1)°, Z = 2, and R = 0.0387 for 5032 reflections where $F_o^2 > 3\sigma(F_o^2)$.

Introduction

The observed oxidation[1] of the linear, trimetallic complex $Au_2Pt(MTP)_4$ (MTP = $CH_2P(S)Ph_2^-$) with halogens to form two new metal-metal bonds in the resultant complexes $Au_2Pt(MTP)_4X_2$ (X = Cl, Br, I) has prompted us to explore the syntheses and chemical properties of related materials. The nearly isostructural $Au_2Pb(MTP)_4$ has been described.[2] It displays a linear metallic array in the solid state with short Au··Au and Au··Pb distances. The MTP anion has been used to form products with various group 10−14 metals.[3,4] These investigations have produced a number of novel species, many of which display interesting structural and/or physical properties, such as extended solid-state linear arrangements,[1,4,5] oxidative addition,[1,4] and photoluminescence.[2,4,5]

The utility of $[Au(MTP)_2]^-$ for the syntheses of bimetallic complexes suggested to us that the neutral, isoelectronic complex, $Hg(MTP)_2$, also might serve as a precursor to the synthesis of bimetallic complexes containing mercury[7] which are analogous to those of gold. We describe here the syntheses, crystal structures, spectroscopy, and a few reactions with the trinuclear heterometallic complexes $[Hg_2Pt(MTP)_4]X_2$ (X = BPh_4^-, PF_6^-). Fenske−Hall type molecular orbital calculations have been performed on these compounds.

Experimental Section

Materials. PPN[Au(MTP)$_2$], Hg(MTP)$_2$, Pt(SEt$_2$)$_2$Cl$_2$, and PhICl$_2$ were prepared according to published procedures.[1] $NaBPh_4$, $TlPF_6$, Br_2, and tetraethylthiuram disulfide, DTC_2, were obtained from Aldrich and used without purification. All solvents were freshly distilled and dried prior to use. All reactions were carried out in Schlenk ware under a nitrogen atmosphere, or in oven-dried NMR tubes where appropriate.

Instruments. ^{1}H NMR spectra were recorded on a Varian XL-200 NMR spectrometer at 200 MHz relative to $(CH_3)_4Si$ (TMS). $^{31}P\{^1H\}$ NMR were also recorded on a Varian XL-200 NMR spectrometer, at 81 MHz relative to 85% H_3PO_4 (external). Cyclic and Osteryoung square wave voltammagrams were measured on a BAS 100 electrochemical analyzer in CH_2Cl_2 (0.1 M $[N(C_4H_9)_4]PF_6$, Aldrich), using platinum working and auxiliary electrodes, with a Ag/AgCl background electrode, referenced against ferrocene, reversible peak at +0.52 V.

$[Hg_2Pt(MTP)_4](PF_6)_2$, 1. To a 1,2-$CH_2CH_2Cl_2$ solution (20 mL) of Hg(MTP)$_2$ (0.100g, 0.15 mol) was added Pt(SEt$_2$)$_2$Cl$_2$ (0.100g, 0.15 mmol) with stirring for 4 h at room temperature. $TlPF_6$ (0.053 g) was added, and a white precipitate (TlCl) began to form almost immediately. After the mixture was stirred for 14 h at room temperature, the precipitate was filtered, and the deep yellow solution was concentrated under reduced pressure and Et_2O was added to precipitate a yellow powder. The product was isolated and recrystallized from 1,2-$CH_2CH_2Cl_2$/diethyl ether (0.097 g, 71% yield based on Hg(MTP)$_2$). The resulting yellow single crystals, $\mathbf{1}\cdot{}^1/_2C_2H_4Cl_2$, allowed structure identification from X-ray diffraction measurements. $\mathbf{1}\cdot{}^1/_2C_2H_4Cl_2$ was found to be soluble in most halocarbon solvents. Mp 220 °C dec. ^{1}H NMR ($CDCl_3$; 298 K): δ_H (CH$_2$) = 2.25 vs TMS; $^2J_{P-H}$ = 12 Hz. $^{31}P\{^1H\}$

* To whom correspondence should be addressed.

[⊗] Abstract published in *Advance ACS Abstracts,* December 15, 1994.

(1) Murray, H. H.; Briggs, D.; Garzon, G. Raptis, R.; Porter, L.; Fackler, J. P., Jr. *Organometallics* **1987**, *6*, 1992.
(2) Wang, S.; Garzon, G.; King, C.; Wang, J. C.; Fackler, J. P., Jr. *Inorg. Chem.* **1989**, *28*, 4623.
(3) Mazany, A. M. Ph.D. Dissertation, Case Western Reserve University, Cleveland, OH, 1984.
(4) Mazany, A. M.; Fackler, J. P., Jr. *J. Am. Chem. Soc.* **1984**, *106*, 801.
(5) Wang, S.; Fackler, J. P., Jr.; King, C.; Wang, J. C. *J. Am. Chem. Soc.* **1988**, *110*, 3308.
(6) Carlson, T. F., Ph.D. dissertation, Texas A&M University, 1992. The product $[Hg_2Pt(MTP)_4](BPh_4)_2$ also is described. It is formed using $NaBPh_4$ instead of $TlPF_6$ in CH_2Cl_2; mp 155 °C dec. It was recrystallized from CH_2Cl_2/Et_2O and characterized crystallographically. Insolubility precluded further study. Anal. Calcd for $Hg_2PtS_4P_4C_{101}B_2Cl_2H_{90}$: C, 54.06; H, 4.01. Found: C, 53.56; H, 4.23. Space group $C2/c$, a = 21.135(9) Å, b = 19.171(9) Å, c = 24.836(6) Å, β = 107.55(4)°, V = 9596(4) Å, Z = 4. The Hg··P··Hg angle is 166.3-(1)° with Hg··Pt of 3.016 (1) Å. The Hg−Pt−Hg angle in this cation is 166.1°. Details are presented in the supplementary materials.
(7) Wang, S.; Fackler, J. P., Jr. *Organometallics* **1988**, *7*, 2415.
(8) Kauffman, G. B.; Cowan, D. O. *Inorganic Syntheses*; Rochow, E. G., Ed.; McGraw-Hill Book Co, Inc.: New York, 1960; Vol. 6, p 211.
(9) Fieser, L. F.; Fieser, M. *Reagents for Organic Synthesis*; John Wiley and Sons: New York, 1967; Vol 1, pp 505−506 and references therein.

0020-1669/95/1334-0426$09.00/0

NMR (CD_2Cl_2; 298 K): δ_P = 49.15 vs H_3PO_4; $^2J_{P-Hg}$ = 53.75 Hz. Anal. Calcd for $Hg_2PtS_4P_6F_{12}C_{53}H_{50}Cl$: 34.21; H, 2.71. Found: C, 34.47; H, 2.87.

Reaction of 1 with $PhICl_2$. $[Hg_2Pt(MTP)_4](PF_6)_2$ (20 mg, 0.011 mmol) was dissolved in $CDCl_3$ (2 mL) in a dry 5 mm NMR tube. Following observation of the initial ^1H NMR spectrum, $PhICl_2$ (3.0 mg) was added to the solution. Spectra were collected subsequently at half-hour intervals over the next 4 h. During this time the initially yellow solution became deep orange, with the formation of a white precipitate. The original doublet (δ = 2.25, ^2J = 12 Hz) diminished greatly within the first three hours, but did not vanish completely, as three new sets of doublets (δ = 1.94, ^2J = 14 Hz; δ = 3.09, ^2J = 11 Hz; δ = 4.03, ^2J = 6 Hz) developed. The reaction appeared to have achieved equilibrium after three hours. The experiment was repeated, this time using 6.0 mg of oxidant, and similar results were obtained. The original doublet vanished completely after only 2 h, and the same three new doublets appeared, but with greater intensity than before. Attempts to crystallize the products resulted in only orange-brown films.

Reaction of 1 with Br_2. Two $CDCl_3$ solutions of $[Hg_2Pt(MTP)_4](PF_6)_2$ (30 mg, 0.011 mmol) were prepared as above in 5 mm NMR tubes. To the first tube was added 1 equiv (0.01 mL) of 1.1 M Br_2 in CCl_4, to the second, 2 equiv of the Br_2 solution. Both were monitored at 30-min intervals for a total of 4 h. A series of singlet and doublet peaks appeared, but overlapped to such an extent that an accurate assignment of shifts or coupling values could not be made. As with $PhICl_2$, the solution became orange with the formation of an off-white precipitate.

Reaction of 1 with PPN[Au(MTP)$_2$]. $[Hg_2Pt(MTP)_4](PF_6)_2$ (50 mg, 0.0276 mmol) was dissolved in 2 CH_2Cl_2 (10 mL) under dry nitrogen. The solution was cooled to −78 °C, and 2 equiv of PPN[Au(MTP)$_2$] (66.1 mg) were added. The resulting mixture was stirred for 2 h during which time a white precipitate formed as the solution color turned from yellow to deep gold orange. The solution was warmed to room temperature and filtered. The filtrate was layered with diethyl ether at 0 °C. In about three days several different crystals appeared, which had colors and habits corresponding to $Hg(MTP)_2$, $(AuMTP)_2$, and $Au_2Pt(MTP)_4$, **2**. These products were identified by ^1H NMR.

Reaction of 1 with Tetraethylthiuram Disulfide, DTC_2. $[Hg_2Pt(MTP)_4](PF_6)_2$ (10 mg, 0.0055 mmol) was dissolved in CH_2Cl_2 (10 mL) under dry nitrogen. To this was added 1 equiv of DTC_2 (1.6 mg). The solution was stirred at room temperature for 24 h. During this time the yellow solution became dark orange. The solvent was evaporated and the remaining orange residue was dissolved in $CDCl_3$ (3 mL) and transferred to a 5 mm NMR tube. ^1H NMR spectroscopy showed several multiplets, in addition to a prominent doublet (δ = 2.31, $^2J_{P-H}$ = 12 Hz) corresponding to the methylene signal of $Hg(MTP)_2$. The identity of this product was confirmed by X-ray crystallography. Several dark orange crystals also formed, but these were unsuitable for X-ray analysis.

Reaction of $Hg(MTP)_2$ with $PhICl_2$. $Hg(MTP)_2$ (30 mg, 0.045 mmol) was dissolved in $CDCl_3$ (4 mL) in a dry 5 mm NMR tube. $PhICl_2$ (12 mg) was added and ^1H NMR spectra recorded at 2-h intervals over the next 6 h. The initial doublet (δ = 2.31, $^2J_{P-}$ = 12 Hz) vanished immediately, as four new doublets appeared (δ = 2.00, ^2J = 13.3 Hz; δ = 2.27, ^2J = 13.3 Hz; δ = 3.02, ^2J = 10.8 Hz; δ = 3.56, ^2J = 13 Hz). This last doublet was observed to vanish with time as a white precipitate formed, while the first three were shifted slightly downfield. The bulk solution became slightly yellow. No crystalline products were isolated.

Metathesis of $Hg(MTP)_2$ with $HgCl_2$ To Form $Ph_2P(S)CH_2HgCl$. $Hg(MTP)_2$ (30 mg, 0.045 mmol) was dissolved in CH_2Cl_2 (5 mL) in a 10 mL test tube. One equivalent of $HgCl_2$ (12.2 mg) was dissolved in 2 mL of CH_3OH and added to this solution. The solution remained clear and colorless for about 1 min, then produced a flocculent white precipitate. This was filtered off, washed with three portions each of CH_2Cl_2, CH_3OH, and diethyl ether, and dried overnight. This product was added to 3 mL of $CDCl_3$, but did not immediately dissolve. The resulting slurry was subsequently stirred at room-temperature overnight, after which the solution was once again clear and colorless. ^1H NMR of this solution showed only one doublet, at 3.08 ppm (J = 10.4 Hz), due to P−H coupling of phosphorus adjacent to a methylene group. Anal. Calcd for $HgC_{13}H_{12}PSCl$: C, 33.4; H, 2.51. Found: C, 32.5; H, 2.50.

Table 1. Crystallographic Data and Collection Parameters for $Hg_2Pt(MTP)_4(PF_6)_2 \cdot {}^1/_2C_2H_4Cl_2$

formula	$C_{53}H_{50}Hg_2PtS_4P_6F_{12}Cl$	Z	2
fw	1860.8	d_{calc} g/cm^3	2.01
space group	$P\bar{1}$ (No. 2)	μ(Mo Kα), cm^{-1}	76.8
a, Å	11.314(4)	radiation (λ, Å)	Mo Kα (0.710 73)
b, Å	13.732(3)	temp, K	293
c, Å	21.019(3)	transm factor:	
α, deg	108.07(1)	max	0.927
β, deg	94.55(2)	min	0.721
γ, deg	94.92(2)	R,[a] R_w[b]	0.0387, 0.0358
V, Å^3	3074(1)		

[a] $R = \sum||F_o| - |F_c||/\sum|F_o|$. [b] $R_w = [\sum w^{1/2}(|F_o| - |F_c|)]/\sum w^{1/2}|F_o|$; $w^{-1} = [\sigma^2(|F_o|) + g|F_o|^2]$.

Crystallographic Data. The single-crystal X-ray analysis[6] of $\mathbf{1} \cdot {}^1/_2C_2H_4Cl_2$ was performed by procedures (Nicolet R3m/E diffractometer, SHELXTL Version 5.1 software) described in detail elsewhere.[10] Crystallographic data and collection parameters are listed in Table 1. Yellow crystals suitable for X-ray diffraction were grown from 1,2-dichloroethane/diethyl ether at ambient temperature. A crystal was mounted on a glass fiber with epoxy. The lattice parameters were determined by using 25 reflections (20° < 2θ < 30°). The data were corrected for Lorentz and polarization effects. Absorption corrections were made empirically on the basis of azimuthal scans. The structure was determined by using Patterson methods and difference Fourier techniques. The final cycles of refinement were performed with hydrogen atoms placed in idealized positions (C−H = 0.96 Å). All non-hydrogen atoms were refined anisotopically except for the 1,2-dichloroethane.

Crystals of $\mathbf{1} \cdot {}^1/_2C_2H_4Cl_2$ are triclinic. The space group $P\bar{1}$ was determined by systematic absences and the successful refinement of the structure. Final residuals were R = 0.0387 and R_w = 0.0358. Atomic coordinates and isotropic thermal parameters for **1** are presented in Table 2. Pertinent bond lengths and angles are given in Table 3.

Molecular Orbital Calculations. Unparameterized Fenske−Hall molecular orbital (FHMO) calculations[11] were performed on the Texas A&M Department of Chemistry's VAX 11/780 computer. The numerical Xα atomic orbital program of Herman and Skillman[12] was used in conjunction with the Xα-to-Slater basis program of Bursten and Fenske[13] to generate basis functions for all the metals. The transition metal atoms assumed $d^{n+1}s^0$ cationic configurations. The basis functions for the metal atom were single ζ except for the d^{10}, which was represented as a double ζ function. A single ζ 6p function with an orbital exponent equal to the atom's 6s exponent was added to complete the metal basis set. For C, P, S, and the halides, the double ζ functions of Clementi[14] were reduced to single ζ functions with the exception of the valence p orbitals, which remained as double ζ functions. Mulliken population analysis was used in the calculations to determine gross and overlap populations, as well as individual atomic charges.

Results reported here are on complexes having non-idealized geometries with the atomic positions taken directly from the crystal data. The positions were orthogonalized to place the first (lefthand) metal atom on the origin for the bimetallic species and the central metal atom on the origin for the trimetallic species. The coordinate system was selected such that the z-axis coincides with the metal−metal axis and the x- and y-axes oriented according to the right-hand rule. In the bimetallic complexes, the positive z-direction on each metal points toward the other metal. For the trimetallic complexes, the positive z-direction on the central metal atom is directed toward the metal on

(10) Porter, L. C.; Fackler, J. P., Jr. *Acta Crystallogr.* **1987**, *C43*, 587.
(11) Hall, M. B.; Fenske, R. F. *Inorg. Chem.* **1972**, *11*, 768.
(12) Herman, F.; Skillman, S. *Atomic Structure Calculations*; Prentice-Hall: Englewood Cliffs, NJ, 1963.
(13) (a) Bursten, B. E.; Fenske, R. F. *J. Chem. Phys.* **1977**, *67*, 3138. (b) Bursten, B. E.; Jensen, R. J.; Fenske, R. F. *J. Chem. Phys.* **1978**, *68*, 3320.
(14) Clementi, E. *J. Chem. Phys.* **1964**, *40*, 1944.

Table 2. Atomic Coordinates ($\times 10^4$) and Isotropic Thermal Parameters ($Å^2 \times 10^3$)[a] for $[Hg_2Pt(MTP)_4][PF_6]_2 \cdot {}^1/_2C_2H_4Cl_2$

atom	*x*	*y*	*z*	U_{iso}[b]	atom	*x*	*y*	*z*	U_{iso}[b]
Pt	3694(1)	1040(1)	2355(1)	30(1)*	C(26)	4913(13)	4313(9)	3399(7)	56(6)*
Hg(1)	1433(1)	2196(1)	2245(1)	39(1)*	C(31)	327(10)	−345(9)	3339(6)	30(5)*
Hg(2)	5925(1)	81(1)	1714(1)	41(1)*	C(32)	−186(12)	−126(11)	3931(7)	55(7)*
S(1)	4825(3)	2226(3)	1982(2)	46(2)*	C(33)	−860(12)	−888(11)	4081(7)	59(7)*
S(2)	2566(3)	−170(3)	2703(2)	41(1)*	C(34)	−1004(12)	−1880(11)	3653(7)	64(7)*
S(3)	4788(3)	1701(3)	3426(2)	41(1)*	C(35)	−504(13)	−2109(11)	3078(8)	74(8)*
S(4)	2592(3)	402(3)	1280(2)	45(1)*	C(36)	141(14)	−1338(11)	2921(7)	73(7)*
P(1)	3889(3)	3443(3)	2083(2)	40(1)*	C(41)	1798(11)	1611(9)	3935(6)	40(5)*
P(2)	1270(3)	619(3)	3144(2)	35(1)*	C(42)	2515(11)	1343(11)	4404(7)	52(6)*
P(3)	6163(3)	838(3)	3350(2)	36(1)*	C(43)	2898(14)	2053(13)	5011(8)	85(8)*
P(4)	3376(3)	−840(3)	782(2)	42(1)*	C(44)	2572(14)	3064(11)	5174(8)	87(8)*
P(5)	937(4)	5409(3)	6768(2)	72(2)*	C(45)	1915(16)	3304(12)	4690(8)	93(9)*
P(6)	8091(4)	7904(4)	961(3)	80(2)*	C(46)	1498(13)	2593(11)	4081(7)	67(7)*
F(1)	1410(23)	5302(11)	6129(7)	297(15)*	C(51)	5744(11)	−490(9)	3323(6)	42(5)*
F(2)	1884(15)	6309(13)	7067(8)	233(10)*	C(52)	4877(13)	−677(11)	3701(7)	63(7)*
F(3)	153(16)	4453(9)	6535(9)	241(11)*	C(53)	4578(14)	−1679(14)	3707(10)	85(10)*
F(4)	329(21)	5634(15)	7361(10)	318(15)*	C(54)	5141(15)	−2467(14)	3322(9)	87(9)*
F(5)	1685(14)	4825(18)	7006(15)	371(22)*	C(55)	6004(14)	−2282(10)	2950(8)	72(7)*
F(6)	254(18)	6117(18)	6611(14)	340(21)*	C(56)	6310(13)	−1273(10)	2947(7)	53(6)*
F(7)	8803(11)	7311(9)	1344(6)	158(7)*	C(61)	7143(11)	1459(10)	4121(6)	39(5)*
F(8)	7397(11)	8518(12)	581(8)	187(10)*	C(62)	7293(13)	1042(11)	4637(6)	56(6)*
F(9)	7735(15)	6899(11)	397(7)	214(10)*	C(63)	8074(14)	1552(11)	5199(8)	71(7)*
F(10)	9141(12)	8207(14)	665(9)	226(13)*	C(64)	8674(14)	2478(12)	5269(8)	76(8)*
F(11)	8400(17)	8883(9)	1542(7)	217(10)*	C(65)	8534(13)	2901(12)	4760(9)	75(8)*
F(12)	6997(14)	7721(15)	1297(10)	255(15)*	C(66)	7773(12)	2402(11)	4175(7)	58(7)*
C(1)	454(11)	1180(9)	2624(7)	45(6)*	C(71)	2654(11)	−1285(9)	−74(6)	42(5)*
C(2)	2368(10)	3086(9)	1748(7)	47(6)*	C(72)	1934(17)	−673(12)	−297(8)	96(9)*
C(3)	6975(11)	797(11)	2635(6)	50(6)*	C(73)	1483(18)	−1009(14)	−968(8)	116(10)*
C(4)	4914(10)	−550(12)	757(6)	58(7)*	C(74)	1624(14)	−1944(12)	−1384(8)	78(8)*
C(11)	4682(12)	4129(10)	1622(7)	47(6)*	C(75)	2329(15)	−2494(13)	−1171(7)	80(8)*
C(12)	4382(15)	3862(11)	938(8)	71(8)*	C(76)	2843(15)	−2186(12)	−494(7)	88(8)*
C(13)	5114(14)	4228(11)	536(8)	75(8)*	C(81)	3142(11)	−1895(9)	1115(6)	43(6)*
C(14)	6157(16)	4877(13)	840(10)	91(10)*	C(82)	1965(12)	−2193(10)	1215(7)	57(7)*
C(15)	6471(15)	5130(12)	1521(10)	77(9)*	C(83)	1774(16)	−3000(12)	1451(9)	80(9)*
C(16)	5748(12)	4754(10)	1898(7)	48(6)*	C(84)	2695(19)	−3510(14)	1605(10)	96(10)*
C(21)	3965(12)	4250(10)	2941(7)	49(6)*	C(85)	3804(17)	−3247(13)	1484(9)	85(9)*
C(22)	3042(14)	4839(11)	3157(8)	76(8)*	C(86)	4054(14)	−2432(10)	1242(7)	66(7)*
C(23)	3095(16)	5469(14)	3818(9)	105(10)*	Cl	9850(8)	4494(7)	859(5)	213(4)
C(24)	4026(17)	5543(13)	4252(9)	110(10)*	C(90)	10381(31)	4704(26)	30(20)	215(14)
C(25)	4986(16)	4976(11)	4053(7)	90(8)*					

[a] Estimated standard deviations in the least significant digits are given in parentheses. [b] For values with asterisks, the equivalent isotropic *U* is defined as one-third of the trace of the U_{ij} tensor.

Table 3. Selected Bond Lengths (Å) and Angles (deg) for $[Hg_2Pt(MTP)_4][PF_6]_2 \cdot {}^1/_2C_2H_4Cl_2$, **1**

Pt-Hg	3.138(1)	Pt-S(2)	2.333(4)
Pt−S(1)	2.327(4)	Pt-S(3)	2.341(3)
Pt−S(4)	2.351(3)	Hg-C(1)	2.08(1)
Hg−C(2)	2.10(2)	Hg-C(3)	2.09(1)
Hg−C(4)	2.11(1)	P(1)-S(1)	2.005(5)
P(2)−S(2)	2.003(5)	P(3)-S(3)	2.013(5)
P(4)−S(4)	2.013(5)	P(1)-C(2)	1.77(1)
P(2)−C(1)	1.76(2)	P(3)-C(3)	1.80(1)
P(4)−C(4)	1.75(1)		
S(2)−Pt−S(1)	178.7(1)	Hg-Pt-Hg(2)	149.1(1)
C(1)−Hg−C(2)	173.0(4)	S(1)-P(1)-C(1)	113.3(4)
S(2)−P(2)−C(1)	113.9(5)		

the righthand side, while this same axis on the two outer metals is aimed back at the central metal. All halides or ligands bound directly to metals were oriented so that their positive *z*-directions pointed toward their respective metal atoms.

Calculations for $[Hg_2Pt(MTP)_4](PF_6)_2$, **1**, were performed based on the dicationic core; no counterion interactions were considered. Linear $Hg_2Pt(MTP)_4^{2+}$ also was modeled using the coordinates of the Au^I complex, $Au_2Pt(MTP)_4$, **2**, replacing Au^I with Hg^{II} at the Au−Pt distance of 3.034(1) Å. Likewise, models of **2** having the bent configuration of **1** were generated by replacing the Hg atoms with Au atoms in each of the two structures. Since the M···Pt distances in these three complexes are nearly alike, the perturbations produced no major changes. The standard C−H internuclear separation of 0.96 Å was used for the methylene groups. To reduce the total number of functions in the calculations, each phenyl group was replaced by a hydrogen atom at the standard P−H distance of 1.42 Å.

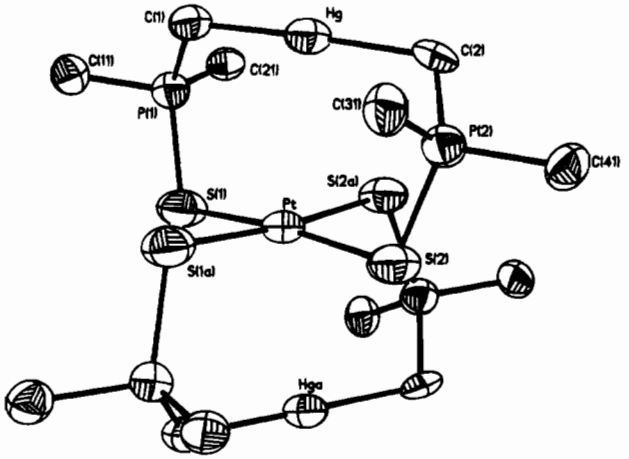

Figure 1. Molecular structure of the cationic core of $[Hg_2Pt(MTP)_4](PF_6)_2 \cdot {}^1/_2C_2H_4Cl_2$ showing 50% thermal ellipsoids.

Results

Structural Information. The skeletal molecular structure of **1** $[Hg_2Pt(CH_2P(S)Ph_2)_4]^{2+}$ is shown in Figure 1. The two mercury atoms are linearly coordinated to the carbon atoms of the MTP ligands, with the platinum atom held in a distorted

square-planar configuration by the four sulfur atoms. The Hg−C distance is 2.11(1) Å. The Pt−S bond lengths are all ca. 2.34 Å with the Pt atom nearly in the plane surface atoms. The P−S and P−C distances are 2.00−2.01 Å and 1.75−1.80 Å, respectively, and the S−P−C angles are between ca. 113°. The Hg···Pt···Hg trimetallic unit is nonlinear[6] with an angle of 149.1(1)°. The Hg···Pt separation is 3.138(1) Å. The hexafluorophosphate anions of **1** are disordered, and the P−F distances were found to lie between 1.37(3) and 1.54(2) Å. A solvent molecule is in the crystal lattice.

NMR Studies. ^{1}H NMR spectroscopy of **1** reveals a doublet, $\delta = 2.25$ with a $^2J_{P-H}$ coupling constant of 12 Hz, typical for a CH_2 group in ylide complexes, as well as two multiplets downfield of 7.0 ppm corresponding to the phenyl resonances. A similar pattern is seen for both[6] $Hg(MTP)_2$ ($\delta = 2.31$, $^2J_{P-H} = 12$ Hz)[7] and $Au_2Pt(MTP)_4$ ($\delta = 1.46$, $^2J_{P-H} = 11.6$ Hz).[1] Faint mercury satellites are detected (^{199}Hg: $I = {}^1/_2$, 16.84% natural abundance), but are so weak that no coupling constant could be assigned. $^{31}P\{^1H\}$ NMR shows a singlet at $\delta = 49.15$ [$Hg(MTP)_2$: $\delta = 44.78$], as well as a septuplet corresponding to the PF_6^- anions. ^{199}Hg and ^{195}Pt satellites appear as a complex multiplet at 49.45 and 48.80 ppm.

In an attempt to determine whether the nonlinear Hg···Pt···Hg core persists in solution, ^{1}H NMR spectra in CD_2Cl_2 were collected, from −60 to +20 °C, at 20 °C intervals. Aside from a slight downfield shift in the doublet position as it becomes better resolved, no changes in the signal were observed. This indicates that the methylene protons are chemically equivalent in solution, and that the nonlinear structure observed in the solid state and for the BPh_4^- salt[6] is not maintained rigidly in solution.

Oxidation of **1** by 1 or 2 equiv of either $PhICl_2$ or Br_2 in $CDCl_3$ at 22 °C rapidly yields orange solutions with a white precipitate which appears to be HgX_2. ^{1}H monitoring of these reactions reveals the disappearance of the parent CH_2 doublet and the concomitant formation of several new peaks. With $PhICl_2$, the original doublet ($\delta = 2.25$, $^2J = 12$ Hz) diminished greatly within the first 3 h, but did not vanish completely, as three new sets of doublets ($\delta = 1.94$, $^2J = 14$ Hz; $\delta = 3.09$, $^2J = 11$ Hz; $\delta = 4.03$, $^2J = 6$ Hz) develop. While these products have not been identified, they are the result of Hg−C bond cleavage.

Reaction of $Hg(MTP)_2$ with $PhICl_2$ also forms a new series of doublets upfield from the initial CH_2 resonance. The white precipitate which forms appears to be $HgCl_2$ and the doublet at $\delta = 3.02$ is assigned Hg(MTP)Cl. Other organic products containing $-CH_2Cl$ apparently also form. The reaction of $Hg(MTP)_2$ with $HgCl_2$ yields the metathesis product Hg(MTP)Cl. ^{1}H NMR of this product reveals a downfield shift in the methylene doublet, from 2.32 to 3.08 ppm.

Ligand Displacement Reactions. The reaction of **1** with DTC_2 (tetraethylthiuram disulfide) results in an orange solution, but unlike the halide reactions, some of the $Hg(MTP)_2$ is removed intact from the platinum center, as determined by both ^{1}H NMR spectroscopy and X-ray crystallography. The orange solution appears to contain various reaction products of DTC with Pt^{II}, including $Pt(DTC)_2$.

The reaction of **1** with 2 equiv of $PPN[Au(MTP)_2]$ was attempted with the thought that a neutral pentanuclear complex might form by coordination of the sulfur atoms of the $[Au(MTP)_2]^-$ to the terminal mercury atoms. Product crystal morphology, unit cell data, and ^{1}H NMR data, however, show that $Au_2(MTP)_2$, $Hg(MTP)_2$, and $Au_2Pt(MTP)_2$ are the major products.

Electrochemical Studies. Cyclic voltammetric measurements of a 5×10^{-5} M solution of **1** show only two irreversible reduction peaks, at −0.78 and −1.08 V (vs Ag/AgCl), with no definite oxidation peaks. This is supported by Osteryoung square wave voltammetry which shows two peaks, at −0.686 and −0.918 V (vs Ag/AgCl). Similar measurements were made of a $Hg(MTP)_2$ solution of roughly equivalent molarity. Two irreversible oxidation peaks were observed at +1.29 and +1.87 V, with no apparent reduction peaks.

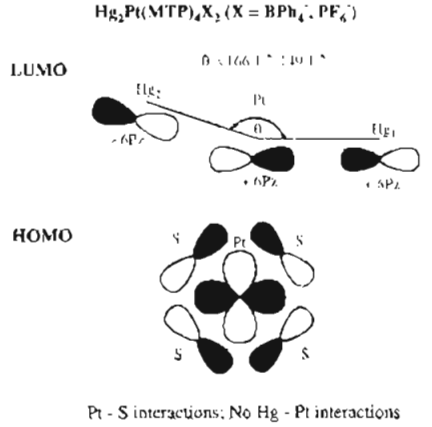

Figure 2. Qualitative HOMO/LUMO representation of the $Hg_2Pt(MTP)_4X_2$ (X = BPh_4^-, PF_6^-) complexes.

Spectroscopy. The UV−visible electronic spectrum of **1** shows a broad absorption band which extends from around 400 nm to well into the UV range. A solid sample of **1** cooled to 77 K luminesces with a bright yellow emission when irradiated with light of 365 nm. A CH_2Cl_2 glass of **1** at 77 K also luminesces, with an orange emission.

FHMO Calculations. Fenske−Hall molecular orbital calculations on these complexes show a major difference in the composition of the HOMO as compared with $Au_2Pt(MTP)_4$, **2**. The FHMO calculations for **2** and its oxidative addition products will be reported[15] elsewhere. They reveal a HOMO in the unoxidized product that is σ antibonding between the $5d_{z^2} + 6s$ orbital combinations on each of the three metal atoms. For $[Hg_2Pt(MTP)_4]^{2+}$ HOMO is 10.1% 6s for each of the two Hg atoms, and 27.6% $5d_{z^2}$ 3.4% 6s for the Pt atom. Qualitative HOMO/LUMO diagrams of the unoxidized and oxidized species are shown in Figure 2. Although no metal−metal bonds are present, interaction along the coincident metal z-axes is apparent. In **2** the Au···Pt distances are equal,[1] (3.034 Å), a distance only slightly shorter than the 3.04 Å separation of the gold atoms in the $[Au(MTP)]_2$ complex.[4] The metal atoms in **2** are rigorously (crystallographically) linear, forming linear chains with an intermolecular Au···Au separation of 3.246 Å. The LUMO is σ bonding between the $6p_z$ orbitals of each metal atom (27.7% for each gold and 29.3% for platinum). The HOMO/LUMO gap is 7.79 eV. Mulliken populations are 1.92 e^- in Au $5d_{z^2}$, 0.81 e^- in Au 6s, 0.099 e^- in Au $6p_z$, 1.82 e^- in Pt $5d_{z^2}$, 0.48 e^- in Pt 6s, and 0.004 e^- in Pt $6p_z$.

In contrast with $Au_2Pt(MTP)_4$, no metal−metal interaction is indicated in the isoelectric $[Hg_2Pt(MTP)_4]^{2+}$. The HOMO of the latter consists of mainly of Pt−S p antibonding interactions, with 10% Pt $5d_{x^2-y^2}$, 49% Pt $5d_{xy}$, and 9% of each of the S $3p_x$ orbitals. The LUMO is similar to the LUMO of $Au_2Pt(MTP)_4$, being almost exclusively σ bonding through interactions of the $6p_z$ orbitals on each metal (16.8% Pt $6p_z$, 27.4% Hg $6p_z$). The Mulliken populations are 1.98 e^- in Pt $d_{x^2-y^2}$, 1.90 e^- in Pt $5d_{xy}$ and Pt $5d_{yz}$, 0.008 e^- in Pt $6p_z$, 0.03 e^- in Hg $6p_z$, 1.49 e in S $3p_x$ and 1.84 e^- in S $3p_y$. The HOMO, shows contributions

(15) Staples, R. J.; Briggs, D. A.; Fackler, J. P., Jr.; Garzon, G.; Hall, M. B.; Murray, H. H.; Raptis, R. G.; Sargent, A. L. To be submitted for publication.

of 51% Pt $5d_{x^2-y^2}$, 5% Pt $5d_{xz}$ and $5d_{yz}$ orbitals, between 2 and 4% of the S $3p_x$ orbitals, and about 7% of the S $3p_y$ orbitals with the ranges reflecting changes in the Hg−Pt−Hg angle from 150 to 180° as observed in the two solid state structures. Pt···Hg interaction is observed, and the HOMO is predominantly π antibonding between Pt and the S atoms. As with the BPh_4^- complex, the LUMO is σ bonding, with Pt $6p_z$, and Hg $6p_z$. When modeled according to the linear structure of the metal atoms in $Au_2Pt(MTP)_4$, the HOMO shows no intermetallic interactions, with 27.8% Pt $5d_{x^2-y^2}$, 31.7% Pt $5d_{xy}$, and 9.2% S $3p_x$. The LUMO is 25.1% Pt $6p_z$, and 36.3% Hg $6p_z$. Mulliken populations are 1.48 e^- in Pt $5d_{x^2-y^2}$, 1.54 e^- in Pt $5d_{xy}$, −0.022 e^- in Pt $6p_z$, 0.06 e^- in Hg $6p_z$, and 1.92 e^- in S $3p_x$. The HOMO/LUMO gap varies from 6.81 to 7.34 eV as the Hg−Pt−Hg angle is changed from 180 to 150°.

The complex $Au_2Pt(MTP)_4$, **2**, also was modeled according to the geometries of the $[Hg_2Pt(MTP)_4]X_2$. Although the extent of Au···Pt interaction decreases with increasing angle, similar HOMO/LUMO characteristics are observed. For a Au−Pt−Au angle of 166.1°, the HOMO consists of σ antibonding interactions between 26.6% Pt $5d_{z^2}$, 3.4% Pt 6s, 9.4% Au $5d_{z^2}$, 9.9% Au 6s, and 1.6% Au $6p_z$ orbitals. The LUMO is σ bonding between 28.8% Pt $6p_z$ and 29.1% Au $6p_z$ orbitals. Mulliken populations are 1.82 e^- in Pt $5d_{z^2}$, 0.48 e^- in Pt 6s, 1.91 e^- in Au $5d_{z^2}$, and 0.017 e^- in Au $6p_z$. When Au−Pt−Au is reduced to 149.1°, the contributions to the HOMO become 15.8% Pt $5d_{z^2}$, 2.8% Pt 6s, 8.1% Au $5d_{z^2}$, and 12.5% Au 6s orbitals. Interestingly, no significant Au $6p_z$ contribution is found at this angle. The LUMO is composed of 27.8% Pt $6p_z$ and 28.3% Au $6p_z$ orbitals. Mulliken populations for these orbitals are 1.89 e^- in Pt $5d_{z^2}$, 0.49 e^- in Pt 6s, 0.018 e^- in Pt $6p_z$, 1.93 e^- in Au $5d_{z^2}$, 0.78 e^- in Au 6s and −0.012 e^- in Au $6p_z$. As the Au−Pt−Au angle is reduced from 180°, the HOMO/LUMO gap increases; 7.79 eV (180°), 7.83 eV (166.1°), and 8.99 eV (149.1°).

Discussion

The reaction of $Hg(MTP)_2$ with Pt^{II} salts leads to trinuclear cationic products, $[Hg_2Pt(MTP)_4]^+$, from which the title compounds have been isolated and structurally characterized. The catonic unit is structurally similar to the isoelectronic $Au_2Pt(MTP)_4$, **2**, complex formed from reactions of $[Au^{II}(MTP)]_2^-$ with Pt^{II} salts.[1] The Hg···Pt distance of 3.138(1) Å is slightly longer than the Au···Pt distance of 3.034(1) Å for **2**; however, the Hg···Pt distance in the BPh_4^- salt is somewhat shorter (3.012 Å). These variations Hg···Pt distances presumably reflect the lack of significant metal−metal interaction in **1** vs **2** (vide infra). The Hg−C distances in **1** are also slightly shorter than the 2.124(6) Å distance for the $Hg(MTP)_2$ molecule.[7] The average Pt···S bond length in **1** compares favorably with the 2.346(5) Å distance observed[1] in **2**. Overall, the geometry of the trinuclear cationic core of **1** is very similar to that of **2**.

The primary structural difference observed between the Au^I and Hg^{II} trinuclear units, $[M_2Pt(MTP)_4]$, is observed in the angle about the Pt^{II}. While the Au···Pt···Au axis in **2** is linear, the Hg···Pt···Hg angle decreases to 149.1(1)° in **1**. This bend which varies with the anion presumably reflects the lack of Hg−Pt bonding interaction and is likely the result of crystal packing forces. The presence of only one methylene doublet in ^1H NMR spectra, down to −60 °C, and a single phosphorus signal in the $^{31}P\{^1H\}$ NMR spectra shows that all CH_2 groups and the four P atoms are equivalent on the NMR time scale. This supports the observation that bending of the Hg−Pt−Hg angle is sensitive to the anion present. In the solid state, the molecules appear to pack most efficiently when the trinuclear core is flexible to bending.

Unlike other recently reported organomercury compounds,[7,16,17] the $[Hg_2Pt(MTP)_4]X_2$ complexes consist of isolated cations rather than an extended polymeric array of **2** and the extended chain neutral gold−MTP complexes, $Au_2(MTP)_2$,[4] $AuTl(MTP)_2$,[2,5] and $Au_2Pb(MTP)_4$.[2] In these latter complexes, short, intermolecular auriophilic contacts are observed between neighboring terminal Au^I atoms.

The absence of extended chain Hg^{II}···Hg^{II} interactions in **1** produces a cation separated by the anions. Catenation in the Au^I complexes is attributed to relativistic effects.[18] Hg^{II} shows reduced relativistic effects compared with Au^I. The absence of an extended chain structure has been noted previously for the two $[AuHg(MTP)_2]PF_6$ isomers.[7]

It is reasonable to assume that the gold 6s and platinum $5d_{z^2}$ valence orbitals are more closely matched in energy than the mercury and platinum orbitals, particularly those along the metal−metal axis. The differences of **1** compared with **2** with regard to halogen oxidative addition are explained as a result. Oxidative addition of X_2 (X = Cl, Br, I) to **2** produces $Au_2Pt(MTP)_4X_2$. In these reactions, the Au^I centers can each be considered to be oxidized to Au^{II}, with the formation of two Pt−Au bonds in the linear X−Au−Pt−Au−X product. The X-ray structure of $Au_2Pt(MTP)_4\ X_2$ shows that single bonds are formed between both gold atoms and platinum, as well as between X and Au. The geometry about each gold atom is consistent with a metal−metal-bonded Au^{II} formalism. The Au−Pt distances[1] are shortened in the bond formation but are rather in sensitive to X, going from 3.034(1) Å in $Au_2Pt(MTP)_4$ to 2.67 Å in $Au_2Pt(MTP)_4X_2$ when X = Cl, 2.68 Å for X = Br, and 2.69 Å when X = I.

In addition to the electronic difficulties associated with Hg^{II}−Pt^{II} bond formation compared with formation of a Au^{II}−Pt^{II} bond, oxidative addition of halogens to the Hg^{II} complex is inhibited by the large ionization potential of Hg^{II} (IP = 34.40 eV) relative to the Au^I (IP = 20.52 eV). The cationic charge also mitigates against oxidative addition. Consistent with the Goddard−Low[20] concept that d^{10} to d^9−s promotion is required for oxidative-addition, such a process is much more difficult to achieve with Hg^{II} than Au^I. Thus failure to form metal−metal bonds because of orbital mismatch and the high promotion energy of the metal ion Hg^{II} appear to influence the chemistry of the trinuclear Hg complexes.

Fenske−Hall calculations on **2** show that a close interaction of metal atoms significantly redistributes the electron density out of the σ antibonding HOMO of **2**, which is composed mainly of interactions between the $5d_{z^2}$ and 6s orbitals of platinum and gold. The LUMO, on the other hand, is σ bonding between the $6p_z$ orbitals of gold and platinum. The partial σ bonding character is carried throughout the linear array of the solid. If $Au_2Pt(MTP)_4$ is modeled according to the geometry of **1** there is no significant change in the composition of either the HOMO or the LUMO. In all three configurations there is about the same Pt $5d_{z^2}$ contribution to the HOMO. The HOMO is consistently σ antibonding with respect to the metal centers, while the LUMO remains σ bonding. There is no evidence that oxidative addition of halogens to $Hg_2Pt(MTP)_4^{2+}$ occurs in the manner observed for **2**. Contour plots of the Pt−S_4 plane

(16) Wang, S.; Fackler, J. P., Jr. *Inorg. Chem.* **1989**, *28*, 2615.
(17) Goodgame, D. M. L.; Williams, D. J.; Winpenny, R. E. P. *Polyhedron* **1989**, *8*, 1913.
(18) (a) Pitzer, K. S. *Acc. Chem. Res.* **1979**, *12*, 271. (b) Pyykkö, P.; Desclaux, J.-P. *Acc. Chem. Res.* **1979**, *12*, 276. (c) Pyykkö, P. *Chem. Rev.* **1988**, *88*, 563. (d) Rosch, N.; Gorling, A.; Ellis, D.; Schmidbaur, H. *Angew. Chem., Int. Ed. Engl.* **1989**, *28*, 1357.
(19) Moore, C. E. *Atomic Energy Levels*; National Bureau of Standards: Washington, D. C., 1958; Vols. 1−3.
(20) Low, J. J.; Goddard, W. A., III. *J. Am. Chem. Soc.* **1986**, *106*, 6115.

show the electron density in both these orbitals to be localized on platinum, whereas it is shared with the terminal gold atoms in **2**. Oxidation by halogens results in the decomposition of **1** in solution to products in which C−Cl bonds result from Hg−C bond rupture. With DTC_2, isolable metal−metal bonded oxidation products also fail to form as the complex decomposes. Initial electron transfer oxidation of a Hg-C bond or the PtS_4 center followed by decomposition appears to best explain the chemistry observed upon halogen addition.

The observed low temperature luminescence of **1** is intriguing. The observed color shift on changing anions is most likely due to MLCT effects,[21] although the structural change in the Hg−Pt−Hg angle may be the origin of the shift observed. A CH_2Cl_2 glass of **1** at 77 K is also color shifted (from yellow to orange) compared with the solid. The origin of the photoluminescence in these MTP complexes is under current investigation.

Acknowledgment. The Robert A. Welch Foundation, the Texas Advanced Research Program, and the National Science Foundation (Grant No. CHE9300107) are acknowledged for financial support. Chris King, Suning Wang, and Xuejun Feng provided helpful discussions.

Supplementary Material Available: Tables of complete bond lengths, angles and anisotropic thermal parameters and ORTEP diagrams for **1** and $[Hg_2Pt(MTP)_4](BPh_4)_2$ (28 pages). Ordering information is given on any current masthead page.

IC9404679

(21) Lees, A. J. *Chem. Rev.* **1987**, *87*, 711.